Methodologies for Computational Studies of Quininoidal Diiminediyls: Biradical vs Dinitrene Behavior

Paul M. Lahti,*,† Andrew S. Ichimura,‡ and Jon A. Sanborn†

Department of Chemistry, University of Massachusetts, Amherst, Massachusetts 01003, and Department of Chemistry, Michigan State University, East Lansing, MI 48824

Received: August 23, 2000

Density functional and post Hartree−Fock ab initio computations were carried out on the lowest singlet, triplet, and quintet states of 1,4-phenylenedinitrene, biphenyl-4,4′-dinitrene, (*E*)-stilbene-4,4′-dinitrene, and (*E*,*E*)-1,4-bis(4-nitrenophenyl)-1,3-butadiene, and (*E*,*E*,*E*)-1,6-bis(4-nitrenophenyl)-1,3,5-hexatriene. Near-degenerate singlet and triplet quinonoidal ground states were found for all systems using CASSCF methodology, with a slight favoring of the singlet, in accord with experimental results. The aromatic quintet dinitrene states lie much higher in energy. Restricted B3LYP hybrid density functional theory (DFT) methods give artifactually high biradical singlet state energies relative to the triplet biradical states, but unrestricted (mixed-state) B3LYP methods correctly give singlet energies that lie somewhat below the triplet state energies, as well as giving geometric results that compare well to the best CASSCF results we could achieve for these biradical states. Appropriate guidelines for selecting CASSCF versus DFT procedures in such cases are suggested in light of comparisons of computed to experimental results.

Introduction

Through understanding exchange interaction in open-shell molecules, one may hope not only to understand molecular bonding better, but also to predict and to control ground-state multiplicity.[1] The *p*,*p*′-dinitrenes epitomize the interplay between π-bond formation and ring aromatization. Studies of these have occurred at intervals since the ground-breaking work of Reiser[2] and Trozzolo et al.,[3] but a rekindling of interest has occurred during the past decade. For example, 1,4-phenylenedinitrene, **1**, has been investigated by UV−vis,[2] cryogenic ESR,[3−5] and recently by Fourier transform infrared (FTIR)[6] spectroscopy. There have also been recent studies of biphenyl-4,4′-dinitrene, **2**,[5a,d,7a−c] and (*E*)-stilbene-4,4′-dinitrene, **3**.[7c−d,8] While spectroscopic investigations have given critical structural and reactivity information about these unusual systems, considerable uncertainty remains concerning the precise natures of their various electronic states.

Computational chemistry can assist with understanding electronic structure and bonding features in systems where experiment cannot give definitive answers. The *p*,*p*′-dinitrenes are excellent targets for such studies, given that they can exhibit multiple electronic states that are not all readily studied by experimental methods. In this article, we describe computational studies of quinonoidal dinitrenes by post-Hartree−Fock and density functional methods. We show that both complete active space self-consistent field (CASSCF) and density functional theory (DFT) give computational results that are in accord with experimental findings, and explore some of the limitations of these methods in reproducing experiment.

Background

The series of dinitrenes **1**−**5**—represented as quinonoidal diiminediyls due to their ground state natures described subsequently—have been generated from diazide precursors **6**−**10**. The photochemical behavior of the aryl diazides is somewhat complex, even if one concentrates only on the spectroscopy of open-shell molecules.[9] UV−vis studies support the production of quinonoidal **1**−**3**,[2] and show that **3** undergoes a gradual dark reaction[8] at 77 K. Electron spin resonance (ESR) studies show biradical triplet state spectra from cryogenic photolyses of all of **6**−**10**.[5,7] Essentially the same biradical spectrum for **1** is produced from **6** in either frozen solution[3−5a,b,d] or crystalline[5c] matrix. The triplet state ESR assignment for **1** is confirmed by hyperfine coupling to two nitrogens found in the triplet-specific half-field transition.[5c] Self-consistent field molecular orbital plus configuration interaction (SCF-MO-CI)

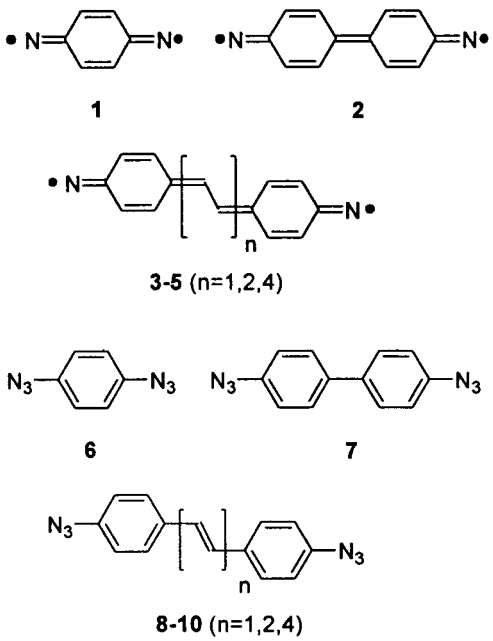

* Author to whom correspondence should be addressed.
† University of Massachusetts.
‡ Michigan State University.

10.1021/jp003040y CCC: $20.00
Published on Web 12/15/2000

computations for quinonoidal triplet state **1** predict a zero field splitting (zfs) in good accord with experiment.[5d]

Also, the triplet ESR spectral intensities derived from **6**−**10** decrease upon cooling to low temperatures. The intensity behavior is reproducible as a function of cycling the temperature between 10 and 70 K, and is attributable to anti-Curie law behavior[1c] from equilibration of triplet biradicals **1**−**5** with slightly more stable, ESR-silent *singlet* state biradicals. This means that UV−vis and IR spectra attributed to **1** are a superposition of singlet and triplet state spectra. The narrowness of the frozen matrix ESR spectra implies an absence of major conformational complexity in the ESR-active species, although in one case[5d] multiple biradical spectra were observed. A slow dark reaction of the ESR-active biradical **3** at 77 K has been described,[8] suggesting reactivity with matrix. No ESR evidence for delocalized dinitrene quintet states has been identified to date.

Cryogenic FTIR studies on the photolysis of **6** were recently carried out by Tomioka's[6] group, who identified not only appropriate vibrational bands assignable to **1**, but those for photorearrangement products accompanying **1**. Assignments were supported by density functional computations that gave good agreement with experiment. A singlet ground state was computed for **1**, in accord with earlier experimental and computational findings.[5] The Tomioka group work showed not only that **1** was photoreactive, but that its IR bands could be effectively assigned by computational methods.

Despite the evidence cited above, various questions remain. The nature of the putative singlet states of **1**−**5** is unclear, since these have not been specifically identified. Likewise, it would be interesting to know how high the unobserved quintet states lie above the related biradical states, since this would be a measure of the energetic interplay between the formation of an extra π-bond in the quinonoidal forms and the presence of aromatic rings in the quintet dinitrenes. The computational studies carried out in this article were aimed at addressing these questions, in addition to delineating the levels of theory that balance the practical limits of computer resources with the need to obtain experimentally verifiable predictions.

Methodology

Multiconfiguration SCF (MCSCF) calculations were carried out with various basis sets using using Gaussian 94 (Revision D.4) or Gaussian 98 for Silicon Graphics workstation computers,[10] GAMESS,[11] Gaussian, or MOLPRO96.[12,13] MCSCF-CASSCF geometry optimizations for the singlet, triplet, and quintet states of **1**−**3** were carried out using standard Pople-type basis sets implemented within the programs. The highest level MCSCF-CASSCF geometry optimizations for the singlet, triplet, and quintet of **1** were carried out using Dunning's [9s5p] basis set[14] with d-orbital polarization on carbon and nitrogen and p-orbital polarization on hydrogen (D95**). For all optimizations, standard tolerances within the programs were used. Some single-point energy computations for **1** were carried out using the D95** and correlation-corrected cc-VTZ(2d,2p) and cc-VTZ(2df,2p) basis sets.[15] All energies reported in this article are given without zero point correction.

For **1**, additional single-point multireference configuration interaction[16] (MRCI) energies were obtained using MOLPRO at the D95** CASSCF(10,10) geometries. The MRCI computations used a six-electron, six-orbital active space; 14 orbitals were designated as frozen core to conform to the limitations of 16 active orbitals inherent to MOLPRO, specifically the eight core orbitals ($3a_g$, b_{2u}, $3b_{1u}$, b_{3g}) and six of the next-lowest

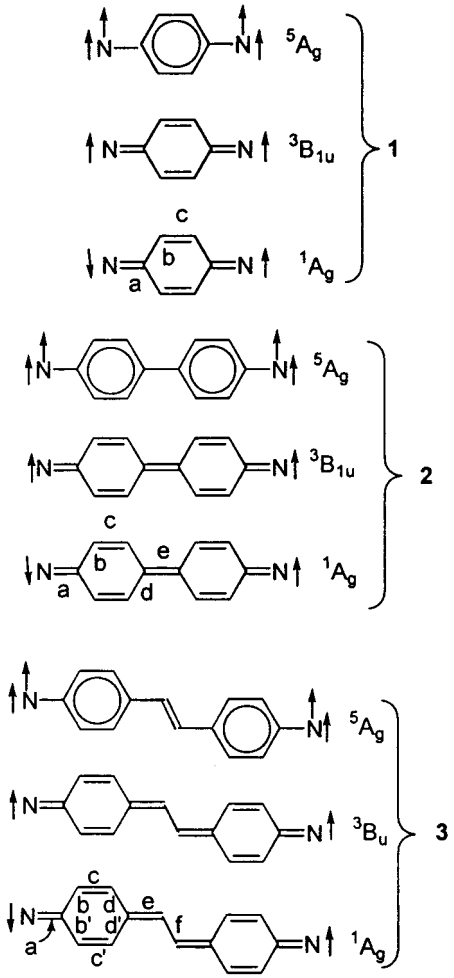

Figure 1. Bonding parameter schemes and states of diiminediyl systems **1**−**3**.

energy orbitals ($2a_g$, b_{2u}, $2b_{1u}$, b_{3g}). The CASSCF(10,10) orbitals[13] were used in the MRCI. The resultant second-order CI wave function correlated 26 valence electrons distributed among 120 virtuals from the 6-electron/6-orbital active space. As part of the MRCI computations, Rayleigh−Schroedinger perturbation theory (RSPT2) energies were also obtained.[17]

CASSCF optimizations for **2** and **3** were carried out using Gaussian or GAMESS with varying standard basis sets within those programs. Where necessary, orbital reordering was carried out to ensure that the same active space orbitals were used for all states in each molecule. Figure 1 shows the states investigated for molecules **1**−**3**. Various data from the computations are summarized in tables in the following sections, as well as in the supporting data section.

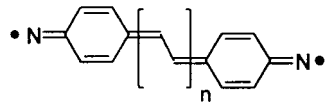

11 (n=3)

Density functional optimizations of singlet, triplet, and quintet states of **1**−**4** and homologous system **11** were carried out with Gaussian using the 6-31G** basis set and B3LYP[18] hybrid DFT wave functions. For the high-multiplicity states, only spin-unrestricted B3LYP (UB3LYP) theory was used, while both spin-restricted (RB3LYP) and spin-unrestricted (UB3LYP GUESS=MIX) methods were tested for singlet states. The

TABLE 1: Computed State Energies for Diradical 1[a]

^1A_g	CAS(6,6)/3-21G	−336.479432	
$^3B_{1u}$	CAS(6,6)/3-21G	−336.479246	(+0.1)
^5A_g	CAS(6,6)/3-21G	−338.445652	(+21)
^1A_g	CAS(8,8)/3-21G	−336.51111	
$^3B_{1u}$	CAS(8,8)/3-21G	−336.50844	(+1.7)
^1A_g	CAS(8,8)/6-31G*	−338.426319	
$^3B_{1u}$	CAS(8,8)/6-31G*	−338.425146	(+0.7)
^1A_g	CAS(6,6)/D95**	−338.439670	
$^3B_{1u}$	CAS(6,6)/D95**	−338.439520	(+0.1)
^5A_g	CAS(6,6)/D95**	−338.387029	(+33)
^1A_g	CAS(8,8)/D95**	−338.464848	
$^3B_{1u}$	CAS(8,8)/D95**	−338.463434	(+1.0)
^5A_g	CAS(8,8)/D95**	−338.419089	(+29)
^1A_g	CAS(10,10)/D95**	−338.514826	
$^3B_{1u}$	CAS(10,10)/D95**	−338.513198	(+0.9)
^5A_g	CAS(10,10)/D95**	−338.457288	(+36)
^1A_g	MR(2,2)CISD/D95**//CAS(10,10)/D95**	−339.029594	
	[RS2(2) corrected]	[−339.16993][b]	
$^3B_{1u}$	CISD/D95**//CAS(10,10)/D95**	−339.029980	(−0.2)
	[RS2(1) corrected]	[−339.16917][b]	(+0.5)[b]
^1A_g	CAS(10,10)/cc-VTZ(2df,2p)//CAS(10,10)/D95**	−338.561589	
	{MR(26)−CISD}	{−339.072848}	
	[MR(26)−CISD/RS2(26)]	[−339.204902][d]	
$^3B_{1u}$	CAS(10,10)/cc-VTZ(2df,2p)//CAS(10,10)/D95**	−338.560077	(+0.95)
	{MR(19)−CISD}	{−339.071259}[c]	(+1.0)[c]
	[MR(19)−CISD/RS2(19)]	[−339.202078][d]	(+1.8)[d]
^5A_g	CAS(10,10)/cc-VTZ(2df,2p)//CAS(10,10)/D95**	−338.500531	(+38)
	{MR(6)−CISD}	{−339.005319}[c]	(+42)[c]
	[MR(6)−CISD/RS2(6)]	[−339.167590][d]	(+23)[d]
^1A_g	UB3LYP GUESS=MIX/6-31G**	−340.405965	⟨1.11⟩[e]
$^3B_{1u}$	UB3LYP 6-31G**	−340.404318	(+1.0) ⟨2.02⟩[e]
^5A_g	UB3LYP 6-31G**	−340.352222	(+34) ⟨6.02⟩[e]

[a] All energies in hartrees without ZPE correction, at geometries optimized at the same level of theory unless otherwise denoted. Numbers in parentheses denote the energy gap relative to the ^1A_g state in kcal/mol. [b] Rayleigh−Schroedinger second-order perturbation theory corrected energy at the corresponding CASSCF/D95** geometry, using a (2,2)-active space. [c] Multi-reference configuration interaction (MR(N)CI) energy using N reference configurations in a (6,6) active space at the corresponding CASSCF geometry. [d] Rayleigh−Schroedinger second-order perturbation theory corrected energy at the corresponding CASSCF/D95** geometry, using a (6,6) active space. [e] Spin-squared expectation value for final eigenstate.

TABLE 2: Bond Lengths for Diradical 1 at Varying Levels of Theory

level of theory	^1A_g	$^3B_{1u}$	^5A_g
CAS(8,8)/3-21G	a = 1.305 Å	a = 1.295 Å	a = 1.428 Å
	b = 1.449	b = 1.460	b = 1.387
	c = 1.338	c = 1.331	c = 1.377
CAS(6,6)/D95**	a = 1.254	a = 1.254	a = 1.408
	b = 1.483	b = 1.483	b = 1.392
	c = 1.348	c = 1.347	c = 1.394
CAS(8,8)/D95**	a = 1.288	a = 1.283	a = 1.403
	b = 1.468	b = 1.473	b = 1.399
	c = 1.337	c = 1.334	c = 1.390
CAS(10,10)/D95**	a = 1.286	a = 1.284	a = 1.389
	b = 1.471	b = 1.473	b = 1.410
	c = 1.353	c = 1.352	c = 1.398
B3LYP[a]/6-31G**	a = 1.276	a = 1.272	a = 1.373
	b = 1.474	b = 1.478	b = 1.416
	c = 1.345	c = 1.342	c = 1.390

[a] UB3LYP GUESS=MIX for singlet state, UB3LYP for high spin states.

results are summarized in figures and tables given in the following sections.

Results and Discussion

Biradical CASSCF Wave Functions for 1—Energy. Tables 1 and 2 show state energies and geometric parameters for **1** at various levels of theory and basis set. The CASSCF results in these tables are discussed in this section, and the DFT results in a subsequent section. Two of us previously carried out an ab initio SCF-MO-CI study of dinitrene **1**,[19] which was hindered by the failure of limited multireference configuration interaction computations at the singles-plus-doubles level (SCF-MO-MRCISD) to give correct energy ordering of the ^1A_g and $^3B_{1u}$, states. Instead, the ^1A_g state was found at various levels to lie 30−230 cal/mol *above* the $^3B_{1u}$ state, in qualitative disagreement with experimental results.[5] The multireference description of the singlet in those computations used the two dominant, doubly occupied configurations with electrons in the nitrogen-centered "lone-pair" type MOs, a MR(2,2)-CISD computation. The triplet computation used only the single corresponding configuration with parallel electron spins. Efforts at partial MRCISD optimization of the two states by manual variation of the C=N and C=C bond lengths did not find significant differences between the states. Inclusion of the Davidson quadruples correction[20] to yield CISD+Q energies at various geometries still did not yield the ^1A_g state below the $^3B_{1u}$ state when up to 30 electrons were correlated in a 52 orbital active space with either the D95** or 6-31G* basis sets.

In the present study, MR(2,2)-CISD computations still give qualitatively incorrect singlet−triplet state ordering relative to the experimental finding of a singlet ground state, even when carried out using our highest level CASSCF(10,10)/D95** optimized geometries (see Table 2). Further refinement of these energies by the Davidson quadruples correction still leaves the singlet state incorrectly higher in energy. However, perturbation theory correction of the MRCISD level energy correctly predicts the state ordering of **1** with a singlet-to-triplet gap of +0.5 kcal/mol. This last approach may in some cases overestimate the stability of the singlet state compared to variational MRCI methods (see discussion below). Still, in general, larger multireference spaces are *required* to compare the singlet and triplet diiminediyl states properly.

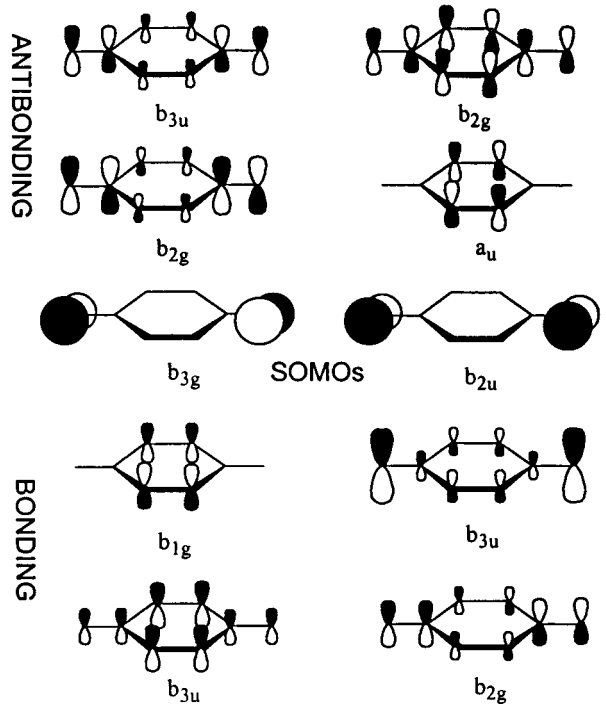

Figure 2. Schematic drawings of active space orbitals used in computations of **1**. For the $^3B_{1u}$ state, the reference state for CASSCF(10,-10) computations was $1b_{3u}^2 1b_{2g}^2 1b_{1g}^2 2b_{3u}^2 4b_{3g}^1 5b_{2u}^1 2b_{2g}^0 1a_u^0 3b_{3u}^0 3b_{2g}^0$.

By comparison to the problems with wave functions having active space insufficiency, we readily reproduced the experimental singlet below triplet ordering of states using fairly crude levels of geometry optimization and limited basis sets, so long as a larger CASSCF active space was used. For example, using a fixed restricted open-shell ROHF/STO-3G* triplet state optimized geometry for all calculations, the $^1A_g-^3B_{1u}$ gap was found to be 1.1 kcal/mol using CASSCF(8,8)/STO-3G* energies. Use of a CASSCF(6,6)/3-21G wave function with separately optimized states yielded a $^1A_g-^3B_{1u}$ gap of 0.1 kcal/mol. If the same or nearly the same quinonoidal geometries are used for both the singlet and triplet states, CASSCF computations with sufficiently large orbital subspaces generally yield a near-degeneracy with a slight favoring of the singlet, in accord with experimental[5] results. We do not mean to imply that the lower level results yield precise information for experimental comparison, but rather to demonstrate that the use of a larger active space is more important than a high level basis set in order to get qualitatively correct state ordering for these biradicals when using CASSCF wave functions.

Our highest level multiconfiguration SCF results using the CASSCF(10,10)/cc-VTZ(2df,2p)//CASSCF(10,10)/D95** level of theory found the $^1A_g-^3B_{1u}$ gap to be 0.95 kcal/mol. The CASSCF(10,10)/D95** ^1A_g ground state is basically a two-configuration wave function, with coefficients of 0.629 and -0.613 for double occupancy of the b_{2u} and b_{3g} molecular orbitals, respectively. The full set of active space orbitals is shown pictorially in Figure 2. The natural orbital occupation numbers for the four frontier orbitals are 1.80, 1.02, 0.98, and 0.21, confirming the two-configuration biradical nature of this state. The $^3B_{1u}$ excited state is largely a single-determinant wave function with a coefficient of 0.886 for its major configuration, single occupancy of both the b_{3g} and b_{2u} orbitals. The natural orbital occupation numbers for the four frontier orbitals are 1.82, 1.00, 1.00, and 0.19 in the triplet state.

Multireference SCF-MO-CI wave functions using MOLPRO gave singlet−triplet energy gaps similar to those of the CASSCF wave functions. MR(6,6)-CI and MR(6,6)-RSPT2 computations with the D95** basis set (MRCISD/D95**//CAS(10,10)/D95**) yielded $^1A_g-^3B_{1u}$ gaps of 1.2 and 2.0 kcal/mol, respectively. For these CI calculations, 26 reference configurations for the ^1A_g state and 19 reference configurations for the $^3B_{2u}$ state were generated within the (6,6) active space. The use of the same active space for single point MRCISD/cc-VTZ(2d,2p)//CASSCF-(10,10)/D95** and MRCISD/cc-VTZ(2df,2p)//CASSCF(10,10)/D95** energies gave $^1A_g-^3B_{1u}$ gaps of 1.1 and 1.0 kcal/mol, respectively. Over 37 million configurations were considered for the ^1A_g state and over 72 million for the $^3B_{1u}$ state in the latter calculations. These are the highest level results attained for **1** in this study. Multireference perturbation computations at the CASSCF(10,10)/D95** geometries with the cc-VTZ-(2d,2p) and cc-VTZ(2df,2p) basis sets yielded energy gaps of 1.9 and 1.8 kcal/mol, respectively. The RSPT2 calculations at all levels appear to overestimate the stability of the ^1A_g state of **1** by about 0.8 kcal/mol in comparison to the variational results and the experimental singlet-to-triplet gap. For the very small energy differences between the quinonoidal biradical states of **1**, variational MRCISD methods are superior for predicting the ground state and magnitude of the energy gap.

ESR Curie law studies of triplet **1** in frozen 2-methyltetrahydrofuran gave singlet−triplet gaps of 574 cal/mol[5d] and 722 cal/mol.[7c] An additional study in which **1** was doped into crystals of *p*-dinitrobenzene recorded a maximum in the triplet spectral intensity at 250 K—well above the maximum attainable in frozen 2-methyltetrahydrofuran—from which a gap of 820 cal/mol was derived.[5c] The latter number is most precise due to the extended temperature range of measurement. Despite the different conditions, the three independent measurements yield similar values of the singlet−triplet gap. The agreement between the highest level computations and experiment is gratifying.

Quintet Dinitrene CASSCF Wave Functions for 1—Energy. Optimizations of the ^5A_g state of **1** at the CASSCF-(6,6)/D95**, CASSCF(8,8)/D95**, and CASSCF(10,10)/D95** levels gave similar geometries (see Table 2). The different active spaces gave $^1A_g-^5A_g$ energy gaps that were comparable in magnitude, with an average value of about 33 kcal/mol (Table 1). MRCISD/D95**//CASSCF(10,10)/D95** level computations with a (6,6)-active space for the quintet state gave a 39 kcal/mol gap. This gap decreased to 21 kcal/mol for a Rayleigh−Schroedinger second-order pertuburbation calculation[22] in MOLPRO using the CASSCF(10,10)/D95** geometry and active space. Virtually the same results are found in comparing the MRCISD to the RSPT2 $^1A_g-^5A_g$ gaps at the cc-VTZ(2df,2p) basis set level. Although there is some variability of the singlet−quintet gaps with the level of theory used, the size of the gaps argues against the quintet state as a thermally accessible intermediate in the 1,4-phenylenedinitrene system, so no further quintet computations were pursued here.

CASSCF Geometries and Bonding in 1. At the CASSCF-(10,10)/D95** level, the triplet and singlet diiminediyl states both have r(C−N) = 1.28 Å, while the quintet dinitrene state has r(C−N) = 1.39 Å. The biradical states have alternating ring bonds of r(C−C) = 1.35 and 1.47 Å, but the quintet state has ring r(C−C) = 1.40−1.41 Å (Table 4). The quintet dinitrene state is considerably more delocalized, an interesting comparison to the more bond-localized geometry recently computed[21] for triplet ground-state phenylnitrene. The latter computations showed bond alternation in the ring (r(C1−C2) = 1.425, r(C2−C3) = 1.386, r(C3−C4) = 1.404 Å) and a relatively short r(C−N) bond of 1.338 Å. These features are due to π-spin

TABLE 3: Computed State Energies for Diradical 2[a]

^1A_g	CAS(6,6)/3-21G	−564.724971	
$^3B_{1u}$	CAS(6,6)/3-21G	−564.724744	(+0.14)
^5A_g	CAS(6,6)/3-21G (D_{2h} geometry)	−564.705452	(+12.2)
^5A	CAS(6,6)/3-21G (D_{2d} geometry)	−564.705214	(+12.4)
^1A_g	CAS(10,10)/6-31G*//CAS(6,6)/6-31G*	−567.946518	
$^3B_{1u}$	CAS(10,10)/6-31G*//CAS(6,6)/6-31G*	−567.946485	(+0.02)
^5A_g	CAS(10,10)/6-31G*//CAS(6,6)/6-31G* (D_{2h} geometry)	−567.908287	(+24.0)
^5A	CAS(10,10)/6-31G*//CAS(6,6)/6-31G* (D_{2d} geometry)	−567.901348	(+28.3)
singlet	UB3LYP GUESS=MIX/6-31G**	−571.448087	⟨1.61⟩
$^3B_{1u}$	UB3LYP/6-31G**	−571.442958	(+3.2) ⟨2.03⟩
^5A_g	UB3LYP/6-31G** (D_{2h} planar geometry)	−571.431760	(+10.2) ⟨6.08⟩

[a] All energies in hartrees without ZPE correction, at geometries optimized at the same level of theory. Numbers in parentheses denote the energy gap from the lowest spin state in kcal/mol. Numbers in carets denote spin-squared expectation value for final eigenstate.

TABLE 4: Bond Lengths for Diradical 2

level of theory	^1A_g	$^3B_{1u}$	^5A_g
CAS(6,6)/3-21G	a = 1.287 Å	a = 1.287 Å	a = 1.428 (1.436) Å[a]
	b = 1.466	b = 1.466	b = 1.388 (1.386)
	c = 1.327	c = 1.327	c = 1.377 (1.381)
	d = 1.470	d = 1.470	d = 1.397 (1.388)
	e = 1.357	e = 1.357	e = 1.494 (1.494)
CAS(6,6)/6-31G*	a = 1.253	a = 1.252	a = 1.395 (1.396)[a]
	b = 1.472	b = 1.472	b = 1.389 (1.391)
	c = 1.327	c = 1.327	c = 1.381 (1.383)
	d = 1.473	d = 1.473	d = 1.397 (1.392)
	e = 1.373	e = 1.373	e = 1.498 (1.499)
B3LYP[b]/6-31G**	a = 1.296	a = 1.278	a = 1.331
	b = 1.453	b = 1.467	b = 1.430
	c = 1.362	c = 1.352	c = 1.382
	d = 1.439	d = 1.454	d = 1.414
	e = 1.429	e = 1.400	e = 1.493

[a] D_{2h} value (D_{2d} value). [b] UB3LYP GUESS=MIX for singlet state, UB3LYP for high spin states.

delocalization onto the 4-position of phenylnitrene. By comparison, the longer C−N bonds and delocalized ring in quintet dinitrene **1** isolate π-spin density on the two exocyclic nitrogens to minimize Pauli repulsion.

Geometric parameters are somewhat affected by the basis set and level of active space. Comparison of the 3-21G and D95** basis sets shows that the structure gets more bond localized with larger, more flexible basis sets. However, the CASSCF(6,6) active space gives C=N bonds that are shorter by about 0.03 Å, and C=C bonds about 0.02 Å longer, than CASSCF(8,8) or CASSCF(10,10) computations with the same D95** basis set. These are not excessively large variations, but show the effects that limited basis set and active space may have in the calculations of larger systems.

Overall, **1** is computed to have a quinonoidal diiminediyl biradical nature with nearly degenerate singlet and triplet states due to isolated electrons in *n*-σ type orbitals. The overall ground state is the ^1A_g biradical. The quintet state of **1** is ≥20 kcal/mol higher in energy, and is not expected to play a significant part in its chemistry. These results are in excellent accord with experimental findings to date for this system. The possibility of aromatization to form the dinitrene is not sufficient to overcome the energetic stabilization of forming an extra π-bond in the quinonoidal form. These findings also correspond closely to results computed by others for *p*-phenylenebis(methylene), **12**, the all-hydrocarbon analogue of **1**. System **12** has been found by CASSCF methods to have a singlet biradical structure with low-lying biradical triplet about 2 kcal/mol higher in energy, and the dicarbene quintet state much higher in energy.[22] Recent experimental and DFT computational studies of **12** by Sheridan's group support this picture of biradical rather than carbene-like behavior.[23]

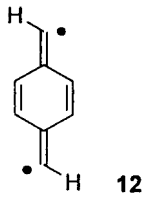

12

Biradical CASSCF Results for 2. The results for **1** guided our treatments of the larger conjugated homologues in this study. A CASSCF(6,6) level of computation was used for optimizing **2** and **3**, using the singly occupied σ-type orbitals plus frontier π-type HOMO and LUMO orbitals in the active space. This was our best active space with the computational resources available to us. Tables 3 and 4 summarize state energy results and bond lengths for the CASSCF and DFT computations on **2**. The CASSCF results are described in this section, and the DFT results are considered in a subsequent section below. The active space orbital subspace of the CASSCF computations is shown schematically in Figure 3.

The biphenyldinitrene system **2** shows interesting experimental behavior. Reiser's UV−vis studies of this system were cited earlier.[2] Yabe's group studied matrix-isolated samples of **2**, interpreting the spectral results in terms of simultaneous generation of both a quinonoidal form and a bisected dinitrene form.[7] By ESR, these workers estimated **2** to prefer a singlet ground state by about 750 cal/mol.[7c] Minato and Lahti estimated[5a,b,d] the gap to be about 580 cal/mol under similar conditions, in reasonable agreement with Yabe's result.

In the present study, both 3-21G and 6-31G* CASSCF(6,6) optimized geometries for **2** show the quinonoidal nature of its lower lying states. The results discussed in this section are those found for the 6-31G* basis set, but summaries of the 3-21G results are found in Tables 3 and 4. Both the ^1A_g ground state and the low-lying $^3B_{1u}$ state have shortened C=N bonds (1.252 Å) and bond-alternating structures. The results for **1** suggest that CASSCF(6,6) active spaces underestimate the C=N bond length somewhat, but not egregiously. Similarly to the results for **1**, the geometries for both triplet and singlet biradical states of **2** are virtually identical. Given the weakly interacting nature of the unpaired electrons in these states, the geometric similarity is understandable.

In a manner similar to the procedure used for **1**, single point CASSCF(10,10)/6-31G*//CASSCF(6,6)/6-31G* energies were obtained for each of the states of **2**. The quinonoidal diiminediyl states are electronically analogous to the corresponding states of **1**. The triplet lies 140 cal/mol higher in energy than the singlet, a value somewhat smaller than the experimental numbers cited at the beginning of this subsection. The ^1A_g ground state is a biradical, as shown by its HOMO and LUMO natural orbital occupancies (1.005 and 0.995) and by the two-configurational

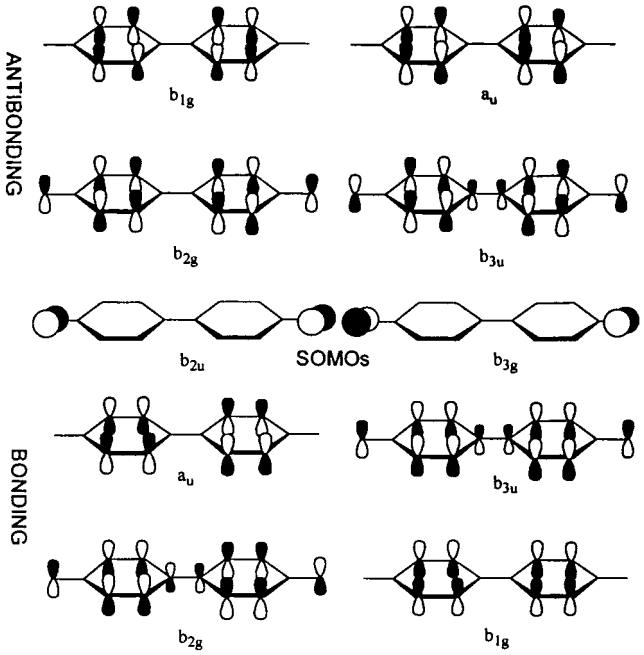

Figure 3. Schematic drawings of active space orbitals used in computations of **2**. For the $^3B_{1u}$ state, the reference state for CASSCF-(10,10) computations was $2b_{2g}^2 1b_{1g}^2 1a_u^2 3b_{3u}^2 8b_{2u}^1 8b_{3g}^1 3b_{2g}^0 4b_{3u} 2b_{1g}^0 2a_u^0$.

nature of its CASSCF(6,6)/6-31G* wave function, for which the dominant configurations are have coefficients of 0.597 and −0.594 for double occupancy of the b_{2u} and b_{3g} orbitals. The b_{2u} and b_{3g} orbitals are of symmetric and antisymmetric *n*-σ type symmetry, as shown in Figure 3. The $^3B_{1u}$ state has frontier natural orbital occupancies of 1.000 for the same SOMOs as the ^1A_g state, and has one dominant configuration of 0.842 with one electron each in the b_{2u} and b_{3g} orbitals.

Quintet Dinitrene CASSCF Results for 2. By comparison to the quinonoidal diiminediyl states, the planar and bisected quintet states of **2** at the same level of theory lie 24 and 28 kcal/mol higher in energy, respectively, and have delocalized structures with fairly long C−N bond lengths (1.395 Å), at least by comparison to the 1.338 Å *r*(C−N) bond length computed[21] for triplet phenylnitrene. The long C−N bonds in quintet **2** are attributable to the desire of the spin density to be localized at opposite ends of the molecule, as in quintet state **1**. The sizable energy gap between the biradical states of **2** and the delocalized quintet states suggests that the latter are unlikely to be present unless they are generated in a metastable condition. However, any bisected quintet state would have to undergo considerable torsion to convert to the quinonoidal states. In the case where Yabe's group postulated[7] a bisected quintet isomer of **2**, perhaps such a species could be generated by a different photochemical route than the planar biradical forms. If so, low-temperature matrix conditions would have to impose a sufficient kinetic barrier to allow the bisected quintet to persist. Given the high-

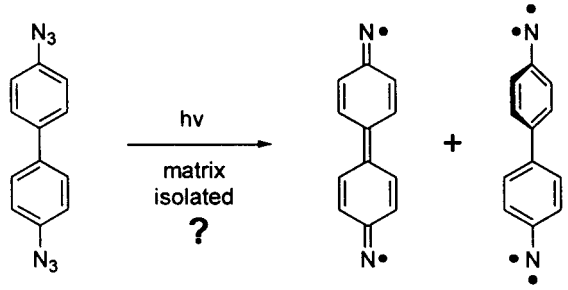

TABLE 5: Computed State Energies for Diradical 3[a]

^1A_g	CAS(6,6)/3-21G	−641.187587	
^3B_u	CAS(6,6)/3-21G	−641.187526	(+0.04)
^5A_g	CAS(6,6)/3-21G	−641.162221	(+16)
singlet	UB3LYP GUESS=MIX/6-31G**	−648.861235	⟨1.52⟩
^3B_u	UB3LYP/6-31G**	−648.856824	(+2.7) ⟨2.05⟩
^5A_g	UB3LYP/6-31G**	−648.847050	(+8.9) ⟨6.09⟩

[a] All energies in hartrees without ZPE correction, at geometries optimized at the same level of theory. Numbers in parentheses denote the energy gap from the lowest spin state in kcal/mol. Numbers in carets denote spin-squared expectation value for final eigenstate.

lying nature of these quintet states, they were not further considered in the analysis of **2**.

Biradical CASSCF Results for 3. Tables 5 and 6 give state energy gaps and computed bond lengths for both CASSCF and hybrid DFT computations on **3**. The CASSCF results are described in this section, while the DFT results will be considered in a later section.

System **3** has undergone fewer detailed studies than **1** and **2**, but has still proven interesting in its own right. It was one of the systems originally studied by Reiser et al.[2] using matrix UV−vis spectroscopy. Minato and Lahti studied its ESR spectroscopy, which showed an excited-state triplet biradical lying 480 cal/mol above a presumed ESR-silent singlet state.[5a,b,d] Yabe and co-workers independently carried out analogous studies, finding similar ESR spectroscopic behavior and estimating a singlet-over-triplet preference of 472 cal/mol.[7c] Harder et al.[8] studied the photochemical behavior of the diazido precursor to **3** by ESR, UV−vis, and FTIR, and found a relatively complex set of reactions that included nonphotochemical hydrogen atom abstraction from the solvent by nitrene reactive intermediates.

The CASSCF(6,6)/3-21G optimized geometries obtained for **3** in the present study show considerable quinonoidal bond localization with nearly degenerate ^1A_g and ^3B_u states. Based on the results described above for **1** and **2**, the effects of a modest-sized basis set and modest six-orbital active space may offset one another in their effects on the bond lengths. The computed singlet-to-triplet gap is 40 cal/mol, smaller than the experimentally observed values but qualitatively correct. The ^1A_g state is a two-configuration biradical with natural orbital occupancy numbers of 1.00 and 1.00. The CASSCF wave function for the ^1A_g state is dominated by two configurations with coefficients of 0.661 and −0.661 for double occupancy of the *n*-σ type b_u and b_g orbitals, respectively. The ^3B_u state has essentially the same active space natural orbital occupancy numbers, but a single dominant configuration of 0.935 with single occupancy of each of the b_u and b_g orbitals. The active space orbitals are shown pictorially in Figure 4. As was true for **1** and **2**, **3** is best described as a localized quinonoid diiminediyl biradical with poor communication between the *n*-σ unpaired electrons on the terminal nitrogens. There is a small preference for the singlet state computationally and experimentally but the geometries and energies of the triplet and singlet biradicals are essentially the same.

Quintet Dinitrene CASSCF Results for 3. For the quintet ^5A_g state of **3**, the active space orbitals shown in Figure 4 were used for CASSCF(6,6)/3-21G computations. The singlet-to-quintet energy gap is 16 kcal/mol. Like **2**, **3** shows a reduced biradical-to-dinitrene energy gap by comparison to that in **1**, presumably due to the fact that the unpaired electrons are further apart in **3** than in **1**. Also similarly to **1** and **2**, quintet **3** has a long *r*(C−N) bond of 1.429 Å and relatively delocalized benzene rings. The planar quintet state basically is a stilbene molecule with long nitrene C−N bonds attached at the para positions.

TABLE 6: Bond Lengths for Diradical 3

level of theory	^1A_g	^3B_u	^5A_g
CAS(6,6)/3-21G	$a = 1.286$ Å $b = 1.471$; $b' = 1.470$ $c = 1.326$; $c' = 1.325$ $d = 1.467$; $d' = 1.468$ $e = 1.343$ $f = 1.445$	$a = 1.286$ Å $b = 1.471$; $b' = 1.470$ $c = 1.326$; $c' = 1.325$ $d = 1.467$; $d' = 1.467$ $e = 1.343$ $f = 1.445$	$a = 1.429$ Å $b = 1.388$; $b' = 1.385$ $c = 1.377$; $c' = 1.380$ $d = 1.395$; $d' = 1.393$ $e = 1.475$ $f = 1.325$
B3LYP[a]/6-31G**	$a = 1.261$ $b = 1.485$; $b' = 1.487$ $c = 1.349$; $c' = 1.349$ $d = 1.451$; $d' = 1.452$ $e = 1.382$ $f = 1.419$	$a = 1.279$ $b = 1.471$; $b' = 1.470$ $c = 1.351$; $c' = 1.351$ $d = 1.452$; $d' = 1.451$ $e = 1.383$ $f = 1.419$	$a = 1.324$ $b = 1.438$; $b' = 1.435$ $c = 1.376$; $c' = 1.379$ $d = 1.418$; $d' = 1.415$ $e = 1.460$ $f = 1.353$

[a] UB3LYP GUESS=MIX for singlet states, UB3LYP for high spin states.

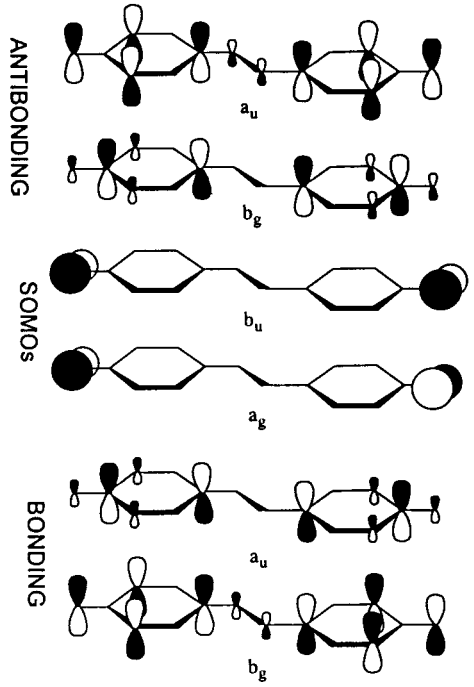

Figure 4. Schematic drawings of active space orbitals used in computations of **3**. For the ^3B_u state, the reference state for CASSCF computations was $4b_g^2 4a_u^2 24a_g^1 24b_u^1 5b_g^0 5a_u^0$.

We did not investigate any nonplanar quintet states of **3**, since these are energetically higher than the planar quintet states, and much higher than the biradical diiminediyl states.

Overall Trends for CASSCF Computations of 1−3. In general, the effect of basis set upon computed singlet−triplet energy gaps for **1**−**3** is less important than the choice of CASSCF active space, if one wishes qualitatively correct ground-state ordering. Since the precision of experimental Curie law measurements is limited by the temperature range of solvent rigidity in most ESR studies, comparisons of experimental and theoretical singlet-to-triplet energy gaps are problematic here (Table 7). A CASSCF(6,6) wave function gives qualitatively correct ordering of state energies and reproduces the small experimental favoring of the singlet over triplet states. The larger active spaces that could be used with system **1** gave good agreement between the computed and experimental singlet−triplet gap. The computations for **2** and **3** all tended to underestimate the singlet−triplet gap relative to the experimental results, but not by a large amount. Flexible basis sets are preferred, especially with polarization, but do not seem critical for proper state ordering.

The computed bond alternation in the Ph−N units of the biradical states of **1** and **3** and phenylnitrene itself[21] is strikingly similar, although phenylnitrene has a large π-spin density that the biradicals do not. This trend suggests that increasing the length of the conjugating polyolefin unit that links the Ph−N units in the series **1**−**5** will not greatly change the CASSCF electronic nature of the Ph−N portions in the diiminediyl, quinonoidal states. As Karney et al.[21] have noted, phenylnitrene has considerable C−N double bond character, making the computed structures of the biradical and the nitrene more similar than might have been expected at first glance. DFT computations described in the next section show the same geometric trend.

The dinitrene quintet state energies are lowered relative to the biradical diiminediyl states for the more conjugated systems **2** and **3**, by comparison to **1** (Table 7). This is attributable to the increased ability of the unpaired electrons in the quintet states to get further away from one another, leading to a decrease in Pauli-type repulsion between electrons with the same spin quantum number. One goal of our experimental studies of **1**−**5** was to determine whether the benzenoid quintet structures could become more stable than the quinonoidal forms.[5] The experiments showed that the quinonoidal biradicals were preferred over the dinitrene states. The present computations argue that the putative quintet dinitrenes will remain sufficiently high in energy not to be thermally populated under cryogenic matrix isolation conditions, even as the conjugating polyolefin gets longer. Geometric torsion in the dinitrenes might give them kinetic metastability, but not much extra thermodynamic stabilization, as shown by results for planar versus bisected **2**. In general, the computations show that torsional deconjugation is only a kinetic means for metastable dinitrene production, not a thermodynamic preference.

DFT versus CASSCF Methodology. Density functional methods offer a way to incorporate electron correlation into a wave function without the complexity and longer run times of the variational post-Hartree−Fock methods. Although DFT has proven useful for treatment of open-shell systems, simpler DFT schemes do not give a proper description of some electronic states.[24] Spin-restricted DFT methods can give badly incorrect triplet−singlet energy gaps for biradicals that have two-configuration singlet excited states, since the spin-restricted DFT methods are basically single determinant in nature.

Unrestricted, mixed-spin state DFT methods have been used elsewhere to study biradicaloid singlet states similar to those treated herein,[24] such as the spectral and computational study of **1** by Tomioka's[6] group. A major drawback of unrestricted DFT methods for treating biradicals is that the singlet state can be very highly spin-contaminated, to the point that a nominal singlet state calculation can yield a 1:1 mixture of singlet and triplet. This spin contamination is exhibited by nonzero values of the spin-squared expectation value, $\langle S^2 \rangle = S(S+1)$, where

TABLE 7: Computed and Experimental State Energy Gap Comparisons for 1−4, 11[a]

	CASSCF S−T gap	DFT S−T gap[d]	experimental S−T gap	CASSCF S−Q gap	DFT S−Q gap[d]
1	0.9 kcal/mol[b]	1.0 kcal/mol	0.57 kcal/mol[e] 0.72[f] 0.82[g]	36 kcal/mol[b]	34 kcal/mol
2	0.02[b]	3.2	0.58[e] 0.75[f]	24[b]	10.2
3	0.04[c]	2.7	0.48[e] 0.47[f]	16[c]	8.9
4	not done	2.6	0.68[e]	not done	7.7
11	not done	2.5	0.14[e]	not done	6.9

[a] All energies are singlet−triplet (S−T) and singlet−quintet (S−Q) gaps in kcal/mol, with the singlet being the lowest state in all cases. [b] CASSCF(10,10) D95** energies for **1** from Table 1, 6-31G* energies for **2** from Table 3. [c] CASSCF(6,6)/3-21G energies for **3** from Table 5. [d] UB3LYP/6-31G** energies from Tables 1, 3, and 5, and Figure 5. [e] Ref 5d. [f] Ref 7c. [g] Ref 5c.

S is the molecular spin quantum number. Strictly speaking, these wave functions are only proper spin eigenfunctions of S_z (not of $<S^2>$), in accord with the typical Pople−Nesbet[25] UHF type formulation.

It can be disconcerting to use such highly spin-contaminated states for singlet state interpretations. The geometric characteristics of higher lying triplet and quintet states may be reflected in the "singlet" state geometry, as the spin contamination increases. But, Davidson has compellingly stated the logic for using the spin-unrestricted DFT methodology for biradical states: "for singlet biradicaloids the only way to get a reasonable potential curve is to follow the UHF philosophy and allow the spin density to be totally wrong. When this is done, however, the UB3LYP potential curve is remarkably close to the true curve in absolute energy".[26] Despite the limitations of unrestricted DFT methods in treating biradical singlet states, they can give geometric and energy results that compare well to experiment, in a less computationally intensive manner than CASSCF methods.[26,27] For the sake of simplicity, in the rest of this section we will refer to spin-unrestricted, mixed-spin state calculations run with a multiplicity of one as being singlet states, even though the wave functions derived from these computations are highly spin-contaminated.

In Tomioka's work,[6] a UB3LYP/6-31G* computation for **1** gave a singlet-to-triplet gap of 1 kcal/mol, in reasonable agreement with the experimental results for **1** and with CASSCF computations undertaken using UB3LYP geometries. The spin-unrestricted singlet wave functions were highly spin-contaminated, being virtually a 1:1 mix of singlet and triplet states based on the spin-squared expectation value. The similarity of the singlet and triplet geometries and frequencies is presumably affected by this high level of spin contamination. Still, experimental FTIR spectra in that study were successfully interpreted using the unrestricted DFT computations.

In the present study, the hybrid B3LYP[18] DFT method was used to compute the various states of biradicals **1**−**3**. In addition, the higher homologues **4** and **11** were investigated, which were prohibitively difficult to treat by the CASSCF methods described in the previous sections. The various DFT results are listed in Figure 5, Table 2, and Tables 4−8. Additional data not given in those tables is given in the supporting material.

A spin-restricted RB3LYP/6-31G** ^1A_g optimization for **1** showed a significantly shorter exocyclic C−N length, 1.241 Å, than the corresponding CASSCF(10,10)/D95** length of 1.286 Å (Table 2). The ^1A_g RB3LYP C−N lengths for **2** and **3** are also appreciably shorter than was found for the corresponding ^1A_g CASSCF computations. All the RB3LYP singlet energies were much higher than the corresponding triplet UB3LYP/6-31G** energies, and were completely unrealistic by comparison to the experimental observations of near-degenerate singlet ground state and triplet excited state. Overall, the restricted spin state results do not seem useful for even a qualitative description of the ^1A_g states of the biradicals **1**−**5**. This is due to the fact that the spin-restricted wave function allows only double

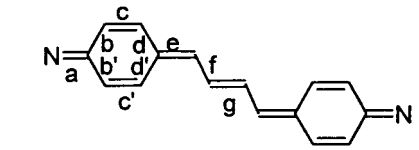

		<S²>
quintet	-726.260636	<6.09>
triplet	-726.268814	<2.06>
singlet	-726.272969	<1.72>

4

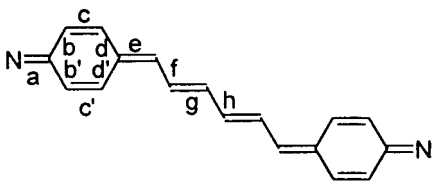

		<S²>
quintet	-803.673376	<6.11>
triplet	-803.680403	<2.00>
singlet	-803.684343	<1.78>

11

Figure 5. UB3LYP/6-31G** energies and selected bonding parameters for **4**, **11**. Energies are in hartrees. Bond length designation letters refer to Table 8. Numbers in carets are spin-squared expectation values. Singlet states were computed using the UB3LYP GUESS = MIX keyword set in Gaussian94 or Gaussian98 (ref 10).

TABLE 8: B3LYP/6-31G Bond Lengths for Systems 4 and 11[a]**

system	^1A_g	^3B_u	^5A_g
4	a = 1.294 Å	a = 1.279 Å	a = 1.320 Å
	b = 1.459; b' = 1.457	b = 1.469; b' = 1.470	b = 1.438; b' = 1.441
	c = 1.360; c' = 1.361	c = 1.352; c' = 1.352	c = 1.377; c' = 1.374
	d = 1.440; d' = 1.438	d = 1.451; d' = 1.452	d = 1.418; d' = 1.421
	e = 1.405	e = 1.382	e = 1.451
	f = 1.399	f = 1.422	f = 1.359
	g =1.394	g = 1.372	g = 1.439
11	a = 1.294	a = 1.280	a = 1.316
	b = 1.457; b' = 1.459	b = 1.470; b' = 1.469	b = 1.443; b' = 1.441
	c = 1.361; c' = 1.360	c = 1.352; c' = 1.352	c = 1.372; c' = 1.375
	d = 1.439; d' = 1.440	d = 1.451; d' = 1.450	d = 1.423; d' = 1.421
	e = 1.405	e = 1.382	e = 1.445
	f = 1.399	f = 1.422	f = 1.362
	g = 1.393	g = 1.370	g = 1.435
	h = 1.401	h = 1.424	h = 1.362

[a] UB3LYP GUESS=MIX for singlet states, UB3LYP for high spin states.

occupancy of molecular orbitals. Since a biradical singlet state requires some orbital occupancy numbers of one, the spin-restricted wave function corresponds to a highly ionic state that is much higher in energy than the biradical state. Further description of the RB3LYP singlet state results is limited to the supporting material.

By comparison, unrestricted spin singlet computations using the UB3LYP GUESS=MIX keywords in Gaussian gave energies much lower than the corresponding RB3LYP energies. All of the unrestricted, mixed-spin state singlets had spin-squared expectation values $<S^2>$ of about 1.0, whereas the expected value should be 0.0. This corresponds to a spin state that is virtually a 1:1 mix of singlet and triplet. But, the mixed-spin state DFT energies are qualitatively much more reasonable than RB3LYP results for the singlet biradicals, despite their strong spin contamination. This is consistent with Davidson's observation, quoted above, that unrestricted DFT wave functions can good singlet biradical energies and geometries, at the expense of very poor spin quantum number descriptions of the state. All subsequent descriptions of DFT singlet state work in this article refer to the results of UB3LYP spin-mixed computations.

The UB3LYP singlet state C−N lengths of **1**−**3** are 1.276, 1.296, and 1.261 Å (Tables 2, 4, 6). In all cases singlet energies lie somewhat below the triplet energies, in qualitative agreement with experiment and the CASSCF results. The singlet−triplet gaps are slightly larger than experiment indicates, but are properly predicted to be small. The triplet state UB3LYP/6-31G** and CASSCF(10,10)/D95** bond lengths all agree to within about 0.01 Å, confirming that DFT optimizations are good alternatives to post Hartree−Fock methods for the triplet state in **1**. The same comparison holds for the more conjugated homologues, judging by comparisons given the tables. The bond lengths for the triplet states of **1**−**3** agree to within better than 0.03 Å for the CASSCF and DFT methods, with the DFT geometries tending to be slightly more delocalized in the ring portions of the structures. Given the success of this comparison, a justifiable procedure to investigate the biradical states of systems such as **1**−**5** would be the use of the triplet UB3LYP/6-31G** geometries for both triplet and singlet, followed by the highest level practically achievable CASSCF computations to evaluate the energy gaps. This, basically, was the procedure used by Tomioka's group.[6]

The agreement of the highest level CASSCF and UB3LYP excited-state quintet geometries for **1** was also encouraging (Table 2). But, for **2** and **3**, the quintet C−N bond lengths at the UB3LYP/6-31G** level are 0.06 and 0.10 Å shorter than those at the highest CASSCF level for **2** and **3**, respectively. This appears to be partly a basis set effect. The CASSCF(8,8)/3-21G geometry for **1** gave a long C−N bond length of 1.43 Å, as was found for **2** and **3** at the CASSCF(6,6) level with the same basis set. The CASSCF C−N bond lengths in **1** decreased by about 0.039 Å going from the 3-21G to the D95** basis set. A change in basis set from 3 to 21G to 6-31G* for the CASSCF(6,6) computation of quintet **3** decreased the C−N bond length by 0.033 Å. This basis set effect was more dramatic in the quintet state than in the corresponding biradical triplet and singlet states. Overall, DFT optimization suggests greater overall localization of geometry in the quintet states than does CASSCF optimization.

The DFT energy gaps between biradical and quintet states for **2** and **3** were significantly smaller than was found at the CASSCF level (Table 7). Although the resources to carry out higher basis set CASSCF computations for the larger molecules were not available to us, the quintet states may deserve more future study. Both DFT and CASSCF results indicate that the quintet states lie sufficiently high above the biradical states to be unobservable under nonmetastable conditions. Table 7 summarizes biradical singlet−triplet (S−T) energy gaps and biradical-to-dinitrene triplet-quintet (T−Q) energy gaps, comparing CASSCF(6,6)/3-21G results for **1**−**3** to corresponding UB3LYP/6-31G** results. The UB3LYP/6-31G** state energy gaps for **4** and **11** are included to complete the structure−property set. The state energy orderings for the CASSCF and DFT methods are the same. Singlet−quintet gaps are substantially larger for the CASSCF method, and singlet−triplet gaps are somewhat larger for the DFT method. Experimental results for the singlet−triplet gaps are in closer accord with CASSCF results than DFT for systems larger than **1**, as is also shown in Table 7. Still, the DFT methodology is in reasonable qualitative agreement with the CASSCF results and with experiment, despite some differences in bonding parameters and state energy gaps. Table 8 summarizes DFT geometric results.

The DFT methodology is also well suited to predicting spin and charge densities. The hyperfine coupling between an unpaired electron and a nuclear spin is related to the Fermi contact integral by the following equation:[28]

$$a_I = (17.023)\left(\frac{16\pi}{3}\right)\left(\frac{g_e g_I}{2}\right) b_F$$

where a_I is the hyperfine coupling constant in gauss for an atom with nuclear spin number I, g_e is the free electron g-value (2.00232), g_I is the g-value for the hyperfine-coupled atom, and b_F is the computed Fermi contact integral. At the UB3LYP/6-31G** fully optimized level for triplet **1**, the predicted hyperfine coupling at the exocyclic nitrogen atoms is 11.2 G, in excellent agreement with the experimental value[5c] of $a_N \sim 13$ G seen in the half-field transition of **1** in solid *p*-dinitrobenzene matrix. By comparison, the UBLYP triplet hyperfine coupling predicted by the same method was only 9.6 G. A number of other density functionals available with Gaussian98 were tested, but UB3LYP gave the best result relative to experiment. Hyperfine coupling is one of few electronic properties for **1** that can be directly probed by our computations, so the agreement supports the application of the UB3LYP DFT method to probe such spin density related electronic properties. The spin contamination of the UB3LYP triplet state is low ($<S^2> = 2.016$) due to the high energy of the quintet dinitrene state of **1**, a factor that is probably important in the good comparison of computational to experimental results.

Summary

Ab initio and density functional computations show that *para*,*para*′ conjugated "dinitrenes" all strongly favor quinonoidal diiminediyl over benzenoid dinitrene states, so thermal detection of the latter under thermodynamic conditions is unlikely under conditions used by experimentalists to date. In **1**−**3**, the singlet biradical quinonoidal state is slightly favored over the triplet, in accord with experimental results. A CASSCF(2,2) wave function is not sufficient for a qualitatively good description of the quinonoidal biradical state energies, but a CASSCF(6,6) with a 3-21G basis set gives reasonably good results. For the computationally most accessible case, **1**, computations with CASSCF(10,10) and MRCI wave functions using higher level basis sets give singlet−triplet energy gaps that are in excellent accord with experimental measurements. CASSCF singlet−triplet energy gaps for higher homologous systems are correctly predicted to be ≤1.0 kcal/mol. Comparison of the experimental

and computational results in **1**—where large active spaces plus large basis sets can be used—to the results for **2** and **3**, indicate that larger active spaces are required for qualitatively correct state ordering, while larger basis sets improve the computed singlet−triplet gap so long as an adequate active space can be achieved.

Density functional computations give an excellent description of the ESR hyperfine coupling in **1** by comparison to the only available experimental benchmark. DFT geometric predictions are in very good accord with those of CASSCF computations for the biradicaloid diiminediyl states, supporting the combination of DFT optimization with CASSCF single point computations for describing similar species. DFT singlet−triplet state energy gaps are rather larger than experiment (1.0−3.2 kcal/mol versus ≤1.0 kcal/mol), but give correct state ordering despite large spin contamination in the spin-unrestricted singlet states. The results justify using unrestricted DFT to probe singlet−triplet biradical energy gaps in cases where CASSCF computations are impractical, while sounding a note of caution concerning the degree of high spin state character that may in some cases be reflected in unrestricted singlet state computations.

Acknowledgment. This work was supported by the National Science Foundation (CHE 9521954 and CHE 9809548). The opinions expressed in this paper are solely those of the authors, and not necessarily those of the Foundation. Support of computing facilities by the University of Massachusetts Graduate School is also gratefully acknowledged. Some computations were carried out at the Michigan State University Department of Chemistry Chemical Visualization Facility.

Supporting Information Available: Summary geometric coordinate data for higher level CASSCF and DFT computations on **1**−**4, 11** (12 pages). This material is available free of charge via the Internet at http://pubs.acs.org.

References and Notes

(1) (a) *Diradicals*; Borden, W. T., Ed.; John Wiley and Sons: New York, 1982. (b) Borden, W. T.; Iwamura, H.; Berson, J. A. *Acc. Chem. Res.* **1994**, *27*, 109−116. (c) Berson, J. A. In *The Chemistry of Quinoid Compounds*; Patai, S., Rappaport, Z., Eds.; John Wiley and Sons: New York, 1988; Vol. 2, pp 462−469. (d) Ovchinnikov, A. A. *Theor. Chim. Acta* **1978**, *47*, 297−304. (e) Klein, D. J. *Pure Appl. Chem.* **1983**, *55*, 299. (e) Michl, J.; Bonacic-Koutecky, V. *Tetrahedron* **1988**, *24*, 7559. (f) Shen, M.; Sinanoglu, O. In *Graph Theory and Topology in Chemistry*; King, R. B., Rouvay, D. H., Eds.; Elsevier: Amsterdam, The Netherlands, 1987; Vol. 51, pp 373−403.

(2) (a) Reiser, A.; Bowes, G.; Horne, R. J. *Trans. Faraday Soc.* **1966**, *62*, 3162. (b) Reiser, A.; Wagner, H. M.; Marley, R.; Bowes, G. *Trans. Faraday Soc.* **1967**, *63*, 2403;

(3) Trozzolo, A. M.; Murray, R. W.; Smolinsky, G.; Yager, W. A.; Wasserman, E. *J. Am. Chem. Soc.* **1963**, *85*, 2526.

(4) Singh, B.; Brinen, J. S. *J. Am. Chem. Soc.* **1971**, *93*, 540.

(5) (a) Minato, M.; Lahti, P. M. *J. Phys. Org. Chem.* **1993**, *6*, 483−487. (b) Minato, M.; Lahti, P. M. *J. Am. Chem. Soc.* **1993**, *115*, 4532−4539. (c) Ichimura, A. S.; Sato, K.; Kinoshita, T.; Takui, T.; Itoh, K.; Lahti, P. M. *Mol. Cryst. Liq. Cryst. Sci., Technol., Sect. A* **1995**, *272*, 279−88. (d) Minato, M.; Lahti, P. M. *J. Am. Chem. Soc.* **1997**, *119*, 2187−2195.

(6) Nicolaides, A.; Tomioka, H.; Murata, S. *J. Am. Chem. Soc.* **1998**, *120*, 11530−11531.

(7) (a) Ohana, T.; Kaise, M.; Yabe, A. *Chem. Lett.* **1992**, 1397. (b) Ohana, T.; Kaise, M.; Nimura, S.; Kikuchi, O.; Yabe, A. *Chem. Lett.* **1993**, 765. (c) Nimura, S.; Kikuchi, O.; Ohana, T.; Yabe, A.; Kaise, M. *Chem. Lett.* **1996**, 125. (d) Nimura, S.; Kikuchi, O.; Ohana, T.; Yabe, A.; Kondo, S.; Kaise, M. *J. Phys. Chem. A* **1997**, *101*, 2083.

(8) Harder, T.; Bendig, J.; Scholz, G.; Stösser, R. *J. Am. Chem. Soc.* **1996**, *118*, 2497.

(9) For general reviews of the chemistry of the nitrenes, see: *Nitrenes*; Lwowski, W., Ed.; Wiley-Interscience: New York, 1970; and Ioffe, B.; Kuznetsov, M. H. *Russ. Chem. Rev. (Engl. Trans.)* **1972**, *41*, 131.

(10) (a) Frisch, M. J.; Trucks, G. W.; Schlegel, H. B.; Gill, P. M. W.; Johnson, B. G.; Robb, M. A.; Cheeseman, J. R.; Keith, T.; Petersson, G. A.; Montgomery, J. A.; Raghavachari, K.; Al-Laham, M. A.; Zakrzewski, V. G.; Ortiz, J. V.; Foresman, J. B.; Cioslowski, J.; Stefanov, B. B.; Nanayakkara, A.; Challacombe, M.; Peng, C. Y.; Ayala, P. Y.; Chen, W.; Wong, M. W.; Andres, J. L.; Replogle, E. S.; Gomperts, R.; Martin, R. L.; Fox, D. J.; Binkley, J. S.; Defrees, D. J.; Baker, J.; Stewart, J. P.; Head-Gordon, M.; Gonzalez, C.; Pople, J. A. Gaussian 94; Gaussian, Inc.: Pittsburgh, PA, 1995. (b) Frisch, M. J.; Trucks, G. W.; Schlegel, H. B.; Gill, P. M. W.; Johnson, B. G.; Robb, M. A.; Cheeseman, J. R.; Keith, T.; Petersson, G. A.; Montgomery, J. A.; Raghavachari, K.; Al-Laham, M. A.; Zakrzewski, V. G.; Ortiz, J. V.; Foresman, J. B.; Cioslowski, J.; Stefanov, B. B.; Nanayakkara, A.; Challacombe, M.; Peng, C. Y.; Ayala, P. Y.; Chen, W.; Wong, M. W.; Andres, J. L.; Replogle, E. S.; Gomperts, R.; Martin, R. L.; Fox, D. J.; Binkley, J. S.; Defrees, D. J.; Baker, J.; Stewart, J. P.; Head-Gordon, M.; Gonzalez, C.; Pople, J. A. Gaussian 98; Gaussian Inc.: Pittsburgh, PA, 1998.

(11) Schmidt, M. M.; Baldridge, K. K.; Boatz, J. A.; Jensen, J. H.; Koseki, S.; Gordon, M. S.; Nguyen, K. A.; Windus, T. L.; Elbert, S. T. *QCPE Bull.* **1990**, *10*, 52 (6 June 1994 version).

(12) MOLPRO version 96.3 (©1996, University of Birmingham, Birmingham, U.K.) is a package of ab initio programs written by H.-J. Werner and P. J. Knowles, with contributions from R. D. Amos, A. Berning, D. L. Cooper, M. J. O. Deegan, A. J. Dobbyn, F. Eckert, C. Hampel, T. Leininger, R. Lindh, A. W. Lloyd, W. Meyer, M. E. Mura, A. Nicklaβ, P. Palmieri, K. Peterson, R. Pitzer, P. Pulay, G. Rauhut, M. Schütz, H. Stoll, A. J. Stone, and T. Thorsteinsson. Werner, H.-J.; Knowles, P. J. See the WWW URL *http://www.tc.bham.ac.uk/molpro/*, "MOLPRO quantum chemistry package", accessed 20 June 1999.

(13) For MCSCF procedures in MOLPRO, see (a) Knowles, P. J.; Werner, H.-J. *Chem. Phys. Lett.* **1985**, *115*, 259. (b) Werner, H.-J.; Knowles, P. J. *J. Chem. Phys*. **1985**, *82*, 5053.

(14) Dunning, T. H. *J. Chem. Phys.* **1970**, *53*, 2823. In the present article, polarization function exponents of $\alpha^{d}(N) = 0.8$, $\alpha^{d}(C) = 0.75$, $\alpha^{p}(H) = 1.0$ were used.

(15) Dunning, T. H., Jr. *J. Chem. Phys.* **1989**, *90*, 1007. In the present article, polarization function d- and f-orbital exponents on carbon and nitrogen were $\alpha^{d1}(N) = 1.654$, $\alpha^{d2}(N) = 0.469$, $\alpha^{f}(N) = 1.093$, $\alpha^{d1}(C) = 1.097$, $\alpha^{d2}(C) = 0.318$, $\alpha^{f}(C) = 0.761$; p-orbital exponents on hydrogen were $\alpha^{p1}(H) = 1.407$ and $\alpha^{p2}(H) = 0.388$.

(16) For MRCI procedures in MOLPRO, see (a) Werner, H.-J.; Knowles, P. J. *J. Chem. Phys.* **1988**, *89*, 5803. (b) Knowles, P. J.; Werner, H.-J. *Chem. Phys. Lett*. **1988**, *145*, 514.

(17) Werner, H.-J. *Mol. Phys.* **1996**, *89*, 645−662.

(18) (a) Becke, A. D. *Phys. Rev. A* **1988**, *38*, 3098−3100. (b) Lee, C.; Yang, W.; Parr, R. G. *Phys. Rev. B* **1988**, *37*, 785.

(19) Ichimura, A. S.; Lahti, P. M. *Mol. Cryst. Liq. Cryst.* **1993**, *233*, 33−40.

(20) Langhoff, S. R.; Davidson, E. R. *Int. J. Quantum Chem.* **1974**, *8*, 61.

(21) Karney, W. L.; Borden, W. T. *J. Am. Chem. Soc.* **1997**, *119*, 1378.

(22) (a) Yamanaka, S.; Kawakami, T.; Okumura, M.; Yamaguchi, K. *Chem. Phys. Lett.* **1995**, *233*, 257. (b) Jean, Y. *J. Mol. Struct. (THEOCHEM)* **1998**, *424*, 29.

(23) Subhan, W.; Rempala, P.; Sheridan, R. S. *J. Am. Chem. Soc.* **1998**, *120*, 11528.

(24) Cramer, C. J.; Smith, B. A. *J. Phys. Chem.* **1996**, *100*, 9664.

(25) (a) Pople, J. A.; Nesbet, R. K. *J. Chem. Phys*. **1954**, *22*, 571. (b) Pople, J. A.; Beveridge, D. L. *Approximate Molecular Orbital Theory*; McGraw-Hill: New York, 1970; pp 51−56.

(26) Davidson, E. R. *Int. J. Quantum Chem*. **1998**, *69*, 241.

(27) Bally, T.; Borden, W. T. In *Reviews in Computational Chemistry*; Lipkowitz, K. B., Boyd, D. B., Eds.; John Wiley & Sons: New York, 1999; Vol. 13, pp 1−97.

(28) Foresman, J. B.; Frish Æ. *Exploring Chemistry with Electronic Structure Methods*, 2nd ed.; Gaussian Inc.: Pittsburgh, PA, 1996; p 136.